Water Resources Research

RESEARCH ARTICLE
10.1029/2023WR034682

Characterizing Space-Time Channel Network Dynamics in a Mediterranean Intermittent Catchment of Central Italy Combining Visual Surveys and Cameras

Simone Noto[1], Nicola Durighetto[1], Flavia Tauro[2], Salvatore Grimaldi[2], and Gianluca Botter[1]

[1]Department of Civil, Environmental and Architectural Engineering, University of Padua, Padova, Italy, [2]Department for Innovation in Biological, Agro-food and Forest Systems, University of Tuscia, Viterbo, Italy

Key Points:

- Field data on the hydrological status of the drainage network are collected via heterogeneous spatiotemporal resolution techniques
- Data are combined to reconstruct the long-term active drainage network dynamics exploiting the hierarchical principle
- The model reproduces the complexity of the non-monotonic pattern of the wet portion of the network in the study site

Supporting Information:

Supporting Information may be found in the online version of this article.

Correspondence to:

S. Noto,
simone.noto@phd.unipd.it

Citation:

Noto, S., Durighetto, N., Tauro, F., Grimaldi, S., & Botter, G. (2024). Characterizing space-time channel network dynamics in a Mediterranean intermittent catchment of central Italy combining visual surveys and cameras. *Water Resources Research*, *60*, e2023WR034682. https://doi.org/10.1029/2023WR034682

Received 16 FEB 2023
Accepted 11 JAN 2024

Abstract Non-perennial streams have a global prevalence, but quantitative knowledge of the temporal dynamics of their flowing length—namely the extent of the wet portion of the stream network—remains limited, as the monitoring of the spatiotemporal configuration of wet channels is challenging in most settings. This work combines the high spatial resolution of visual surveys and the high temporal resolution of camera-based approaches to reconstruct the space-time stream network dynamics in a 3.7 km^2 Mediterranean catchment of central Italy. Information on the hydrological status of the stream network derived from 40 field surveys and sub-hourly images collected with 21 stage-cameras are combined exploiting the hierarchical principle. The latter postulates the existence of a Bayesian chain, defined from the local persistence of the nodes that dictates their wetting/drying order during expansion/retraction cycles of the flowing stream network. Our results highlight the complexity of network dynamics in the study area: while the number of wet nodes decreases during the dry season and increases during the wet season, the local persistency exhibits a highly heterogeneous non-monotonic spatial pattern, originating a dynamically disconnected network. Despite this heterogeneity, the hierarchical model well approximates the temporal evolution of the state of the network nodes, with an accuracy that exceeds 99%. Crucially, the model allows the reconstruction of the wet portion even in cases in which part of the network was not observed. This work provides a novel conceptual approach for the reconstruction of the wet portion of the network in poorly accessible sites.

1. Introduction

Non-perennial watercourses are rivers or streams that periodically cease to flow somewhere along their network. Within this definition, the terms "intermittent" and "ephemeral" refer, respectively, to those streams in which surface flows are generated by both precipitation and groundwater, or solely by precipitation (Busch et al., 2020). In this work, we used the term "IRES," which stands for Intermittent Rivers and Ephemeral Streams (Costigan et al., 2017), and the term "non-perennial" (Busch et al., 2020) referred to a watercourse that periodically cease to flow. We used the term "temporary" only referred to those points of the stream network that experienced such dynamic (see Section 3). IRES can be observed across a variety of climate settings from humid headwater catchments (Botter & Durighetto, 2020; Larned et al., 2010) to dryland regions (Tooth, 2000) and represent a major fraction of the global river network (Costigan et al., 2017; Datry et al., 2014; Messager et al., 2021). In the last few decades, the interest of the scientific community in non-perennial rivers increased and gave rise to several studies on the hydrological, biogeochemical, and ecological function of IRES which also provided a novel view on the relevant conservation, restoration and policy issues (Leigh et al., 2016). Empirical studies conducted across many regions of the world described how the drainage networks of rivers and streams do not occupy predefined portions of the landscape, but expand and contract in response to seasonal climate variations and individual rainstorms (e.g., Durighetto et al., 2020; Zanetti et al., 2022). Many recent works focused on the development of theoretical and modeling tools for the description of such dynamical behavior (Botter & Durighetto, 2020; Botter et al., 2021; Durighetto & Botter, 2022; Godsey & Kirchner, 2014; Jensen et al., 2018; Lapides et al., 2021; Prancevic & Kirchner, 2019; Senatore et al., 2021; Serrano-Notivoli et al., 2022). The change in spatiotemporal extent of drainage networks affects ecosystem services provided by IRES (Pastor et al., 2022; Stubbington et al., 2020) and on key river ecological functions, for example, carbon and nutrient cycling, in-stream biogeochemical processes, hyporheic exchange and biotic communities (Banegas-Medina et al., 2021; Burrows

et al., 2017; Datry et al., 2014; Durighetto et al., 2022; Giezendanner et al., 2021; Gómez-Gener et al., 2021; Larned et al., 2010; Miliša et al., 2022; Sarremejane et al., 2021; Steward et al., 2022).

The interrelationships between multiple abiotic and biotic factors that characterize complex environments, such as the IRES, makes monitoring and managing these systems particularly challenging (Borg Galea et al., 2019). Field surveys are the common method to monitor the intermittence of streamflow and the implied changes in the flowing network extension (Durighetto et al., 2020; Godsey & Kirchner, 2014; Jensen et al., 2017), even though these surveys are highly time consuming. Several alternative methods to map flow intermittency have been also proposed, such as overland flow detectors (Kirkby et al., 1976; Vertessy & Elsenbeer, 1999; Zimmermann et al., 2014), temperature sensors (Constantz, 2008), electrical resistance (ER) sensors (Peirce & Lindsay, 2015; Zanetti et al., 2022), uncrewed aerial vehicles (Micieli et al., 2022), remote sensing (Borg Galea et al., 2019; Spence et al., 2015; Tulbure et al., 2022) and time-lapse imagery using cameras (Herzog et al., 2022; Kaplan et al., 2019). A combination of such techniques has been also used in a few instances to detect temporal patterns of active network extension (Assendelft & van Meerveld, 2019; Kaplan et al., 2019). However, the main issue in remote flow detection techniques concerns the identification of zero-readings (Herzog et al., 2022; Zimmer et al., 2020) and the problem of integrating technologies with different spatial and temporal resolutions has not been fully addressed by the existing literature.

In this work we combine field surveys and digital cameras, two techniques that are characterized by different spatial and temporal resolutions, to reach the following goals: (a) reconstruct the spatiotemporal dynamics of the stream network in a Mediterranean catchment; and (b) test and identify the hierarchical structure of the observed dynamics. The hierarchical principle that underlies stream network dynamics, first introduced by Botter et al. (2021), enables the identification of the unique set of active network configurations that can be observed during the complex expansion-retraction cycles experienced by IRES. This principle allows the prediction of the state (wet vs. dry) of the entire stream network based on the observed state of a subset of strategic nodes. Consequently, it provides a useful tool for the characterization or modeling of stream network dynamics and can significantly facilitate the field mapping of IRES in difficult-to-access environments. While the value of the hierarchical structuring of stream networks has been already discussed by previous studies, the potential of the hierarchical model to integrate heterogeneous data sources on stream network dynamics has been poorly investigated.

The research questions addressed in this paper are the following:

1. How can we combine heterogeneous information on surface flow presence, gathered via different techniques to extrapolate observational data in space and time, and then reconstruct network dynamics in case of missing information?
2. What are the distinctive characteristics according to which stream drying and wetting dynamics take place in a small headwater catchment with a Mediterranean climate?

These questions will be addressed by combining experimental data and theoretical tools, with specific reference to the Montecalvello field site, which is a small non-perennial Mediterranean catchment located in central Italy.

2. Materials and Methods

2.1. Study Site

The selected site for this study is the Montecalvello catchment, located in central Italy, about 30 km north-east of Viterbo (Figure 1b). The drainage area at the outlet is 3.73 km^2 and the elevation ranges from 130 to 340 m a.s.l. The stream mainly runs south-eastward through ravines, where the highest slopes of the catchment are observed. According to Corine Land Cover 2018 (Figure 1c) the catchment is mainly covered by heterogeneous vegetation types: a broad-leaved forest (19%) is found in riparian areas around the geomorphic stream network, while olive groves (41%), vineyard (5%) and other crops (35%) are observed in the plateaus and the parts of the basin where the slope is gentler. According to the Geological map of Lazio region, the dominant lithology is represented by the class "tufa, diatomite, and clays" (67%) which is observed in the plateaus and in the north-western branches of the stream network. Gravel and conglomerates are found mainly in the riparian zone (22%), while travertine is observed in the north-eastern plateaus (11%) (Figure 1d).

This site belongs to the Mediterranean climatic region, based on the calculation of the ombrothermic index for the summer quarter (Ios3), which is defined as the ratio between the cumulated rainfall in mm (during the period

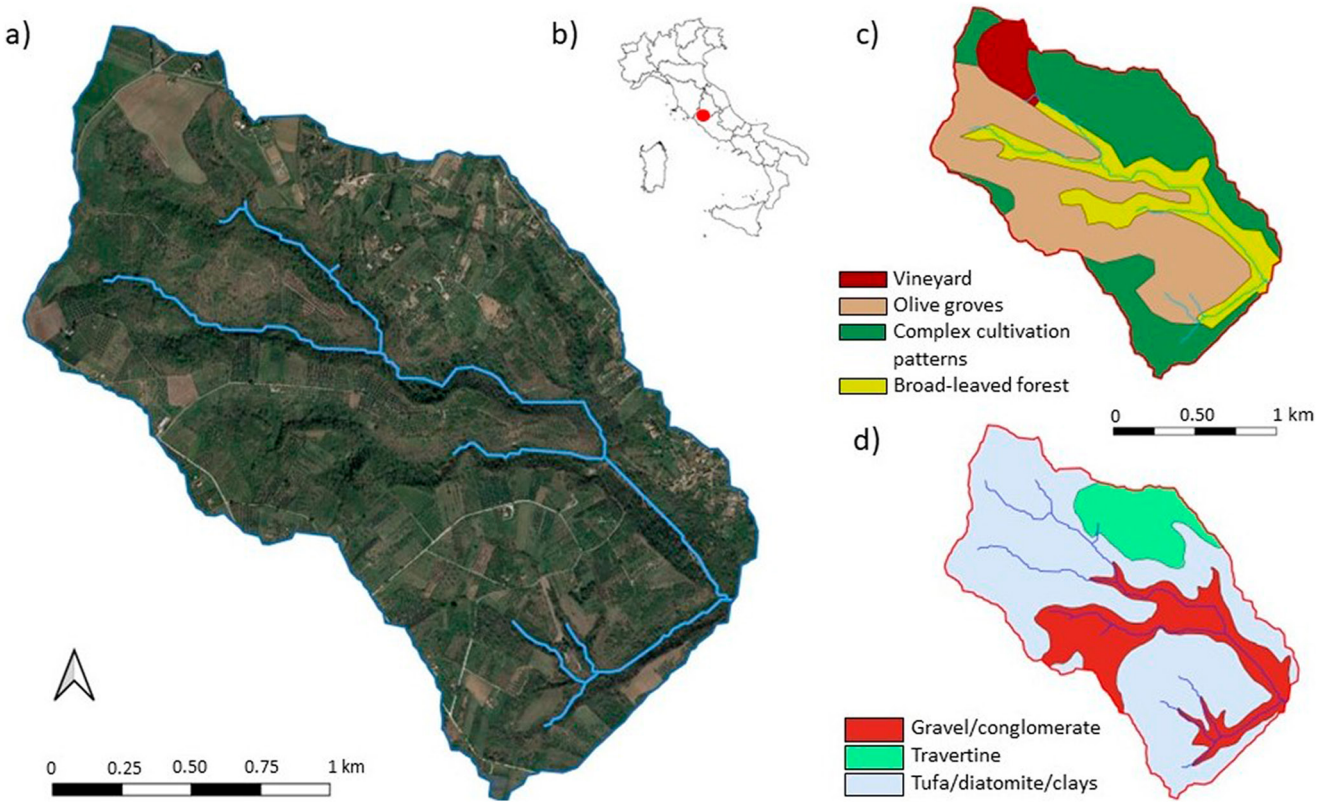

Figure 1. (a) Orthophoto of the Montecalvello catchment and geomorphic stream network (blue line). (b) Montecalvello catchment location. (c) Land cover according to Corine Land Cover 2018. (d) Lithology according to the regional Geological map.

from June to August) and the sum of the monthly mean temperature in Celsius degrees during the same period (Ios3 = 1.42 in this case) (Rivas-Martínez et al., 2011). The climate of the study catchment is characterized by relatively high precipitation throughout spring and fall, and dry summers (from June to August). The mean annual rainfall is 903 mm, and the mean annual temperature is 14.2°C. These statistics were obtained from the available daily weather data collected between 2004 and 2022 by the nearest weather station of the SIARL (Servizio Integrato Agrometeorologico della Regione Lazio) located in Bagnoregio Castel Cellesi, 4 km far from the catchment centroid. To gather local data during the study period, a weather station 0.75 km east of the outlet of Montecalvello catchment was installed. It has been active since 10 March 2020 and the logging time was 10 min. We compared the 2020–2022 rainfall data from the Montecalvello weather station to the averaged long-term rainfall timeseries from Bagnoregio weather station (Figure S1 in Supporting Information S1). Except for winter 2021 and summer 2020, the seasonal observed rainfall amounts were below the corresponding long-term average. Moreover, observed rainfall dynamics highlighted a generic decreasing trend of the monthly rainfall depth during the study period (Figure S2 in Supporting Information S1), especially for the summer season. A significant decrease in the seasonal rainfall depth occurred both in the winter and summer of 2022 as compared to 2021, while a slighter reduction was observed in the spring. Thus, the site experienced particularly dry conditions during the last part of the study period.

2.2. Active Drainage Network Mapping

To map the drainage network, we conducted field surveys between October 2019 and August 2022 and installed 21 stage cams (Noto et al., 2022) in correspondence of strategic nodes since June 2021 to cover the period from June 2021 to August 2022. At the beginning of the mapping surveys all the stream segments and the catchment hillslopes were visited by trained researchers (who explored the Montecalvello catchment during the 3 years of the study period), also taking into account their accessibility. Then, the geomorphic network (i.e., the fixed domain of the potential network) was defined by merging the ensemble of the streams meeting at least one of the

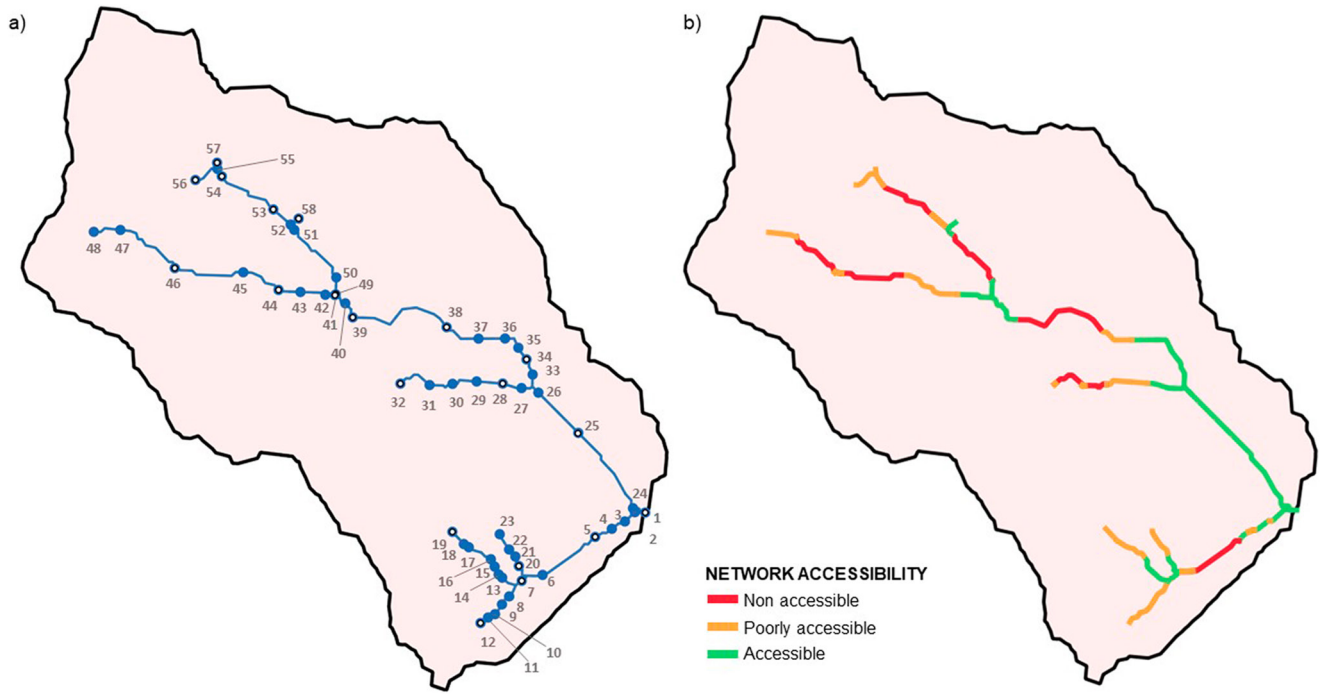

Figure 2. Monitoring nodes and network accessibility. (a) Monitoring nodes progressively numbered downstream-upstream and clockwise at each confluence; white dots represent the nodes monitored by cameras. (b) Accessibility of the network. Here, the accessibility refers to the overall accessibility of the streams.

following conditions: (a) presence of flowing water during at least one or more surveys; (b) presence of permanent channelization signs (Durighetto et al., 2020). Though being aware of the biological importance of pools and standing water along the network (Vander Vorste et al., 2020), we treated the status of each stretch as a binary random variable with two possible states (wet or dry, see Section 2.3). In particular we considered as wet only the segments which experienced flowing water with a wet width of at least 10 cm, while we considered as dry the stream with no water and the streams with ponds or stagnant water in line with previous studies carried out in similar frameworks and with analogous goals (Botter et al., 2021; Durighetto et al., 2020; Ilja Van Meerveld et al., 2019; Senatore et al., 2021). The analysis was conducted by conceptualizing the whole stream network using 58 reference nodes (Figure 2a). The nodes were used to subdivide the network into a number of stretches. In particular, in this case we considered a stretch as a section of the drainage network which embeds the node (Botter et al., 2021). The density and the distribution of the nodes (hereafter monitoring nodes) varied along the network to better capture the dynamic of the active length: the higher the spatial variability, the higher the density of the nodes. Figure 2 depicts the spatial distribution of the 58 monitoring nodes of the Montecalvello catchment. Some portion of the network were characterized by a poor accessibility. This did not enable the monitoring of the stream segments between node 5 and 6, 38 and 39, 45 and 46, 46 and 47, 50 and 51, 53 and 54. The initial nodes placement was decided during the first 15 surveys based on the spatial heterogeneity of observed flow properties and morphological attributes, as mentioned above, while the entire network inspection at daily scale was possible just in a few cases, when the visual surveys were combined with the cameras observation (see Section 2.2.2). The stretch length associated to each monitoring node and the mean distance between the nodes are displayed in Table S1 of the Supporting Information S1. The table indicates that each node represent a stretch with a variable length, and an average length of about 100 m.

2.2.1. Visual Surveys

The wet/dry state of the stream has been visually surveyed (Figure 3) from October 2019 to August 2022, walking along the geomorphic stream network of the Montecalvello catchment and providing a KML map of 58 nodes, through the android app Geo Tracker, and relative observed status during each survey as per the procedure identified by Durighetto et al. (2020). The spatiotemporal resolution of the visual surveys was affected by the limited accessibility of the site. The number of nodes that were monitored during an individual survey increased with time (from a few nodes per survey to the whole set of 58 monitoring nodes) as deeper knowledge of the

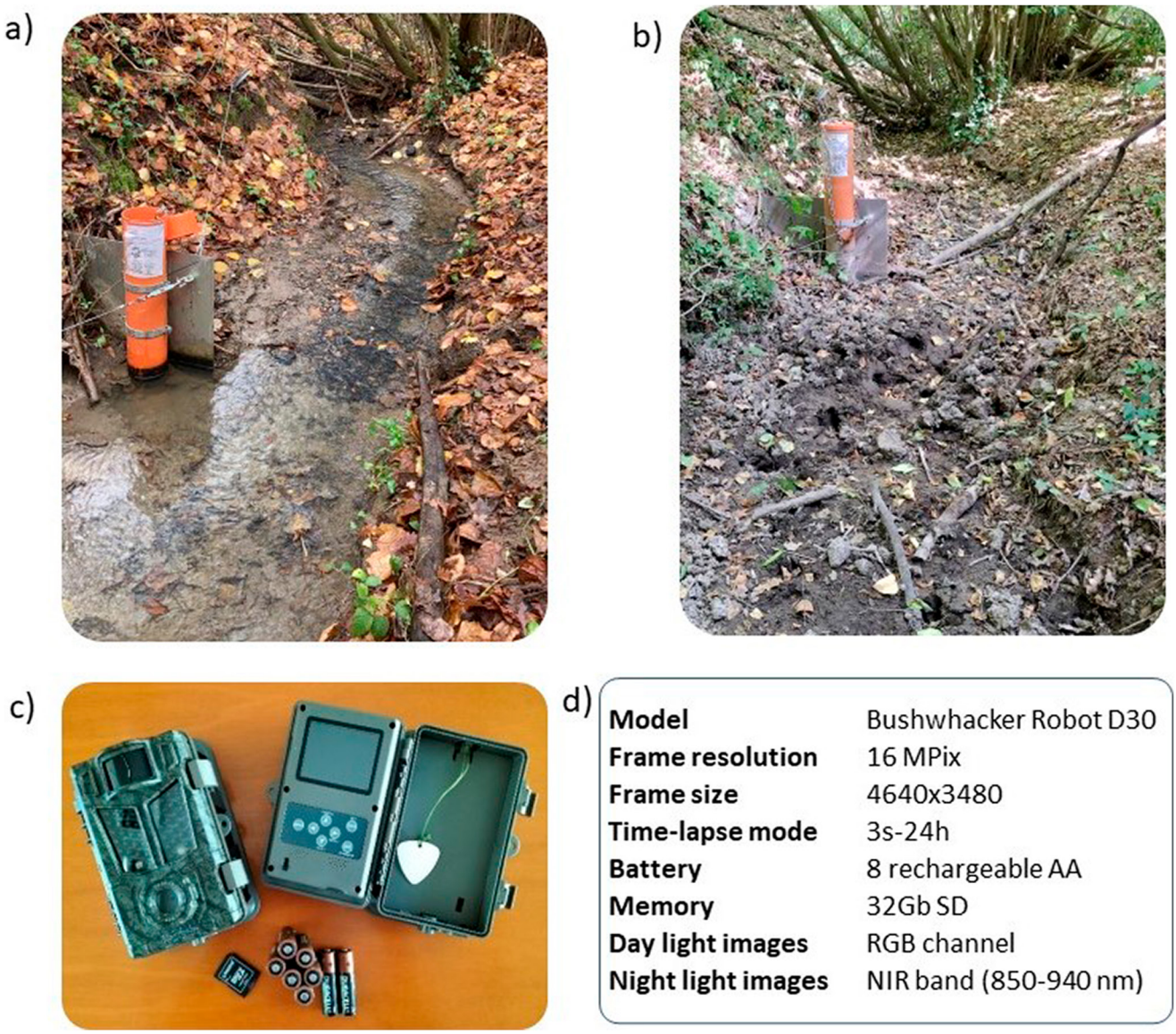

Figure 3. Example of visual surveys carried out at node 34: (a) fall and (b) summer. (c) Wildlife camera trap used in this work and (d) summary of the specifics.

drainage network and morphology of the basin turned in quicker surveys. Moreover, some of the visual surveys were carried out during the pandemic period due to Covid-Sars 19. These circumstances led to a low temporal resolution of the available data during certain periods. In what follows, N_f defines the number of nodes monitored by field surveys with a biweekly/monthly time resolution ($N_f = 58$).

2.2.2. The Camera Network

To enhance the temporal resolution of the visual surveys, a monitoring method based on a network of Camera Traps was also used. A similar method has also been proposed for the monitoring of non-perennial streams (Kaplan et al., 2019). The stage-camera system proposed in Noto et al. (2022) and Tauro et al. (2022) were tested at node 34 of the actual monitoring network and then, the camera network was installed. The cameras selected for this application were the same ones of the referenced works. The 32 Gb SD card and the 8 Duracell rechargeable AA batteries used in this study ensured a running period of 1 month before requiring maintenance. Moreover the cameras were covered with a plastic gable roof (50 cm × 50 cm) to prevent poor image quality due to rainsplash effect.

The camera-based network consisted in 21 monitoring stations along the stream network, with a relative distance between cameras of about 270 m (Table S1 in Supporting Information S1). The main practical issue for the

Table 1
Summary of Data Sets: Number of Nodes for Each Technique and Time Resolution

		Inspection	N° of nodes	Temporal resolution
Observed	N_f	Visual	58	Biweekly/monthly
	N_c	Cameras	21	20 min
	N_{tot}	Observed	58	From 20 min to biweekly/monthly
Merged data set	N_{tot}	Merged	58	Daily

Note. N_f stands for nodes monitored by field surveys; N_c stands for nodes monitored by cameras; N_{tot} stands for total of the monitoring nodes.

installation was the accessibility of the stream network. The camera nodes were set downstream at each accessible confluence and nearby the most accessible heads with a nearly homogeneous distance along the tributaries and the channel of main stream (Figure 2). Some cameras were installed in locations in which flowing water occurred only during heavy rainfall events. To capture this phenomenon the camera monitoring network acquired images with a 20 min time resolution.

In what follows, N_c denotes the number of nodes monitored by cameras ($N_c = 21$). The position of the cameras corresponded to 21 of the 58 nodes monitored by the visual surveys. The cameras were active from 6 June 2021 to 30 August 2022. The number of cameras grew from 16 to 21 during the study period. Since 30 September 2021 all the cameras of the monitoring network were installed. Due to some technical issues (e.g., low battery) the number of nodes in which the cameras collected useable images ranged between 11 and 21 per day. During the study period, the mean percentage of cameras for which no information was available on the daily status of the nodes was 14.5%.

2.3. Exploiting the Hierarchical Principle to Combine Data Sets With Heterogeneous Spatial and Temporal Resolutions

In our framework, the stream network was represented by a set of $\boldsymbol{N}$ nodes, where each node i ($i \in (1, N)$) identifies a uniform stretch of a stream length. The dynamic of the stretches could be represented by a time-dependent state $\boldsymbol{X_i}$, which can be interpreted as a Bernoullian binary random variable. The presence ("*wet*") or absence ("*dry*") of flowing water corresponded to $\boldsymbol{X_i} = 1$ and $\boldsymbol{X_i} = 0$ respectively. $\boldsymbol{P_i}$ is the probability of the node i to be wet, and it is termed local persistency (Botter & Durighetto, 2020):

$$P_i = \text{Prob}\,[X_i = 1] = E[X_i] \tag{1}$$

The local persistency was calculated from the observed data as number of surveys in which the node i was wet over the total number of surveys:

$$P_i = \frac{n^\circ \text{ wet observations}}{n^\circ \text{ total observations}} \tag{2}$$

The active drainage network length is expressed as:

$$L(t) = \sum_{i=1}^{N} \Delta l_i \, X_i(t) \tag{3}$$

where $L(t)$ is the length of the active drainage network at a given day t, Δl_i is the length of the stretch associated with the node i.

In this work, two different data sets with contrasting spatiotemporal resolutions were merged (Table 1). The aim of this section is to define a procedure to combine this dual information and optimize the description of stream dynamics in complex settings of the type investigated here.

The features of the two data sets to be merged can be summarized as follows:

- N_f nodes visually surveyed n_f times with biweekly/monthly time interval
- N_c nodes surveyed by cameras n_c times with 20 min time interval

The merged data set is represented by a number of nodes that is equal to:

$$N_{tot} = N_f \cup N_c \tag{4}$$

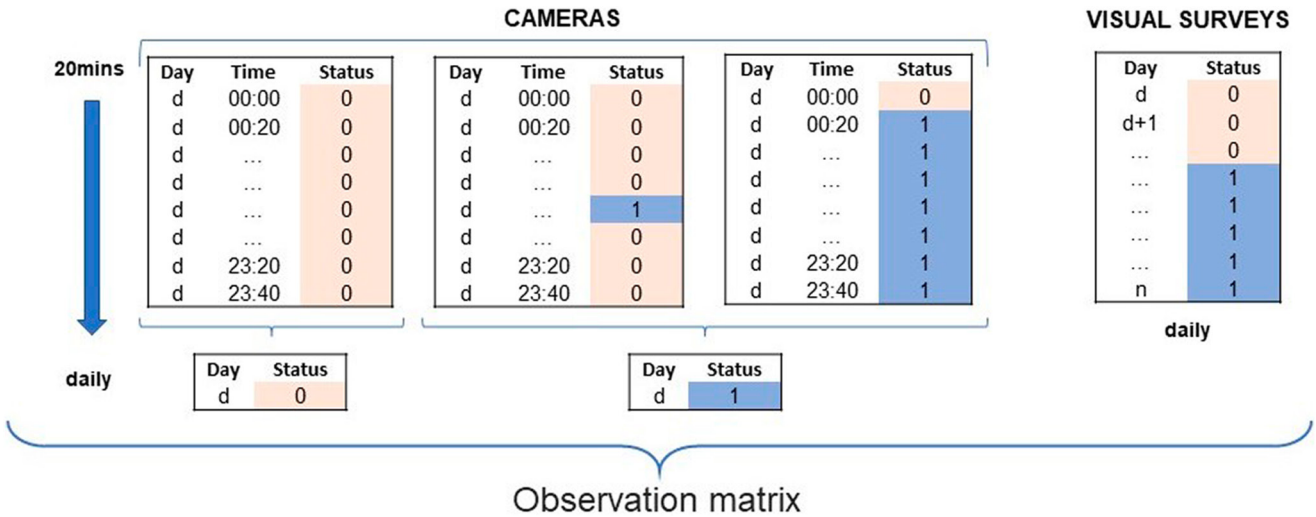

Figure 4. Merging data set scheme. Sub-hourly data from cameras were converted to daily information to match the information from the visual survey: a given node *i* was considered wet (1) during the day *d* if flowing water was detected in at least one frame captured by camera or if it was detected during the visual survey. Opposite, the node *i* during the day *d* was considered as dry (0). The result of the data set merging was the observation matrix.

where $N_{tot} = 58$ is the total number of nodes surveyed by either field surveys or cameras. In this case $N_{tot} = N_f$ as the nodes surveyed by cameras correspond to a subset of the nodes surveyed by visual inspection (Table 1).

The state of a node (X_i) represents the hydrological condition of the node during the day in which field survey was performed, or the state of the node when the image was taken by a camera, depending on the data source. Thus, a suitable homogenization of the data resolution was needed to merge the two data sets. The data from the cameras consisted in 72 snapshots per day. To convert this sub-hourly information to a daily information, a node *i* that experienced flowing water at least in one frame captured by the camera during a given day was considered wet in that day (Figure 4). This choice was done to capture quick variations of the state of a node in response to short rainstorms.

Let us define n_{tot} as the number of days in which at least one node of the network was surveyed:

$$n_{tot} = n_f + n_c - n_{f\_Over} \tag{5}$$

where n_f and n_c represent the number of days, in which the nodes were monitored by field surveys or cameras respectively, while n_{f_Over} represents the number of times in which both camera-derived and field mapping-derived data were gathered. The merged data set consisted in N_{tot} nodes observed n_{tot} times (in this work $N_{tot} = 58$ and $n_{tot} = 480$). The observation matrix was made up of N_{tot} columns and n_{tot} rows and was built as follows. The assignment of the state X_i of the nodes depends on the data availability during each day of the study period. If the nodes were observed only by visual survey, the states X_i corresponded to the states of the N_f nodes. This is the case for all the observations pertaining the period before the installation of the cameras. If the nodes were observed only through cameras, the states X_i corresponded to the state of the N_c nodes as derived from the analysis of the snapshots taken by the cameras during that day. This happened in the time periods in between two visual surveys. In case of missing information, for example, due to maintenance issues, the gaps (X_i = NaN) were filled with the field survey derived information if it was available. Otherwise, "NaN" was assigned to the states of all the nodes with missing information. An excerpt of the observation matrix is depicted in Supporting Information S1 (Figure S3).

The observation matrix represented the input for the hierarchical model. The hierarchical principle postulates that the nodes can be ordered in a Bayesian chain (Koski & Noble, 2011) based on their local persistency and this chain of nodes dictates the order of activation/deactivation during expansion and retraction cycles (Botter & Durighetto, 2020). The chain in this case was built as follows: for each couple of nodes, *i* and *j*, the number of times in which *i* was wet while *j* was dry, N_{ij}, and the number of times in which *j* was wet and *i* was dry, N_{ji}, were calculated. If $N_{ij} > N_{ji}$, the node *i* precedes the node *j* in the chain (hierarchy). If $N_{ij} = N_{ji}$ (except for $N_{ij} = 0$ and $N_{ji} = 0$) the nodes were considered synchronous. The procedure was repeated for each couple of nodes. In

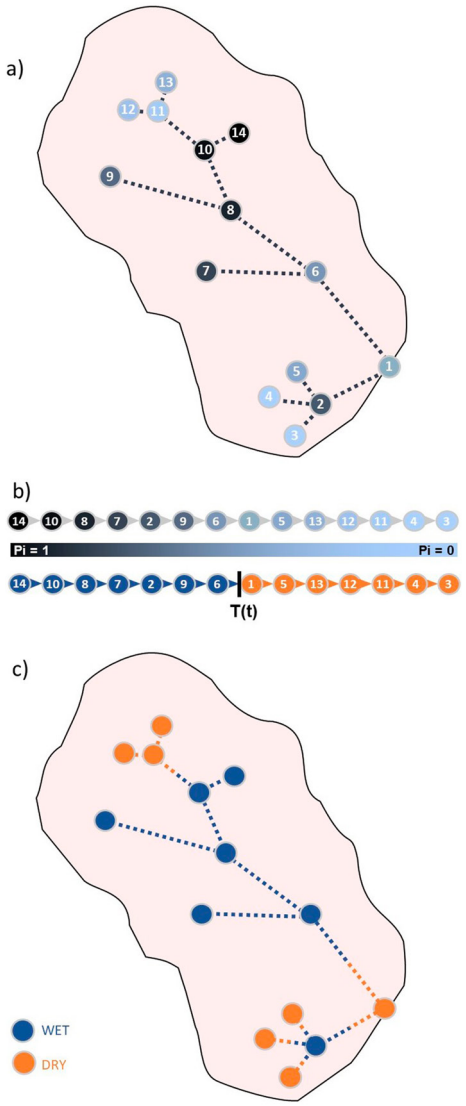

Figure 5. (a) Schematic representation of the main stream and of the tributaries of the Montecalvello catchment: the nodes connected in the physical space are colored in shades of blue, representing the hierarchy of the nodes. (b) The nodes, in shades of blue, are reordered in a chain that reflects the hierarchy, from the most ($\boldsymbol{P}_i = 1$) to least persistent ($\boldsymbol{P}_i = 0$); the threshold $T(t)$, represented by the black line, separates the wet nodes from the dry nodes. (c) Example of the state of the stream network reconstructed based on the position of the threshold along the chain.

case of loops, they were removed based on the more robust statistic information (e.g., retaining only the information associated to the higher value of $|N_{ij} - N_{ij}|$). In this way the nodes were connected in a probabilistic space. Two nodes connected in the probabilistic space were not necessarily connected each other in the physical space. In Figure 5 a schematic representation of the hierarchy of the stretches of Montecalvello is depicted. Notably, some couples of neighboring nodes in the physical space (e.g., node 7 and 6, 2 and 1, 5 and 2), were not directly connected in the probabilistic space.

If the observed network dynamics were strictly hierarchical, the resulting chain would correspond to all the nodes of the network reordered from the most to the least persistent, (from $\boldsymbol{P}_i = 1$ to $\boldsymbol{P}_i = 0$). If the hierarchical principle holds, the hierarchy dictates the activation and deactivation order of the nodes. Thus, the wet nodes can be separated from the dry nodes by a time dependent threshold $T(t)$ along the chain (Figure 5). This principle allowed the reconstruction of the states of the nodes which were not observed in the field. The threshold is represented by a specific node, which is identified as the middle point in between the last observed wet node and the first observed dry node along the chain. The "distance" between such nodes corresponded to the threshold uncertainty and reflected the uncertainty in the positioning of the threshold in cases in which not all the nodes were observed at the same time. Threshold uncertainty decreased with time: values upper than 10 nodes occurred before the installation of the camera network, while values equal to 0 can be found mainly in a set of surveys at the end of the study period. Surveys in which the uncertainty was more than 20 nodes, that were the 0.43% of the total number of surveys, were not considered in the reconstruction of the dynamic, to avoid misleading interpretation of the model owing to the uncertainty associated to the observational data.

The accuracy of the hierarchical model (Equation 6) was obtained by the comparison of the observed states of the nodes to the hierarchical order in each date of survey (that was every date in which the nodes were observed by visual surveys, by the network of cameras or both):

$$\text{Accuracy} = \frac{\text{TP} + \text{TN}}{\text{TP} + \text{TN} + \text{FP} + \text{TP}} \tag{6}$$

Therein, TP (true positive) and TN (true negative) corresponded respectively to the number of nodes and times in which the model correctly estimated the states of the nodes, FP (false positive) and FN (false negative) corresponded to the cases in which the model was not able to correctly classify the state of a node. Moreover, the nodewise and the timewise accuracy were calculated. The nodewise accuracy represented the mean accuracy of the model at each node while the timewise accuracy represented the mean accuracy of the model during a given day.

3. Results

The temporal trend of activation/deactivation of the nodes at Montecalvello catchment followed a seasonal behavior as implied by the Mediterranean climate of the site. In Figure 6 the reconstruction of the extension of the active drainage network during the study period is shown. Blue and orange represent the TP and the TN respectively. TP and TN values mean that the model correctly classified the state of the nodes. Contrarily, FP (in red) and FN (in dark blue) represent the surveys or nodes in which the modeled states did not fit the observed state. The expansions and contractions of the network, during the fall and the summer clearly appear. In fact, the number of wet nodes decreased as the season got dryer and vice versa: the modeled number of nodes ranged from 16 (summer of 2020) to 51 and 41 (January 2021 and January 2022 respectively). The maximum number of wet nodes was equal

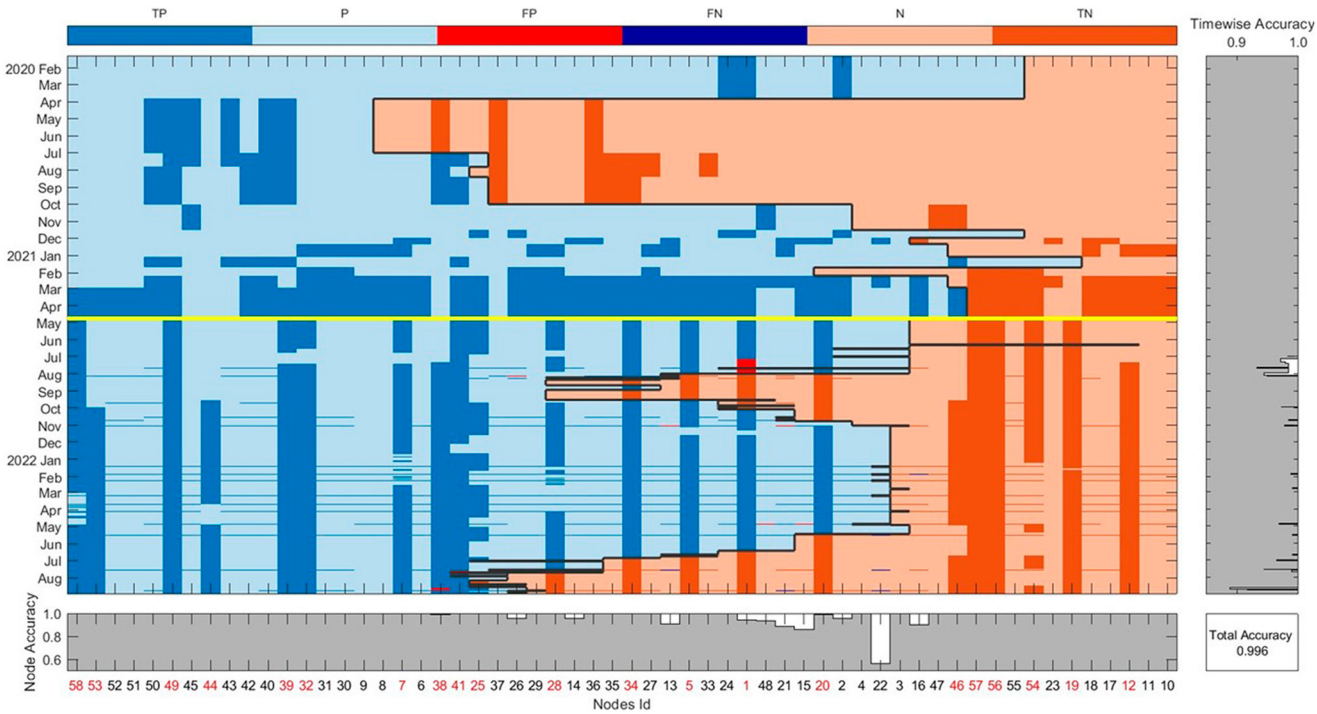

Figure 6. Comparison between the status of the nodes reconstructed by the model and the state of the nodes observed during field surveys and by cameras from January 2020 and August 2022. The nodes are ordered according to the hierarchy chain. The plot has been split in status of the nodes observed only by field surveys before the installation of the cameras (above the horizontal yellow line) and status of nodes observed by combined field surveys and cameras (below the horizontal yellow line). The black line represents the threshold T(t), which define the extension of the active drainage network, estimated by the model. The shades of blue represent the wet nodes: correctly classified wet node (TP), classified wet node (P) and wrongly classified dry node (FN). The shades of red represent dry nodes: correctly classified dry nodes (TN), classified dry node (N), wrongly wet classified nodes (FP). The red numbers represent the nodes monitored by cameras below the yellow line.

to 56 during a heavy rainfall event (summer of 2021). The minimum and maximum modeled extent of the active drainage network corresponded to 1.750 and 5.860 km respectively. Of notice that a more relevant contraction was observed during the summer of 2020, but during such period, a low number of nodes were monitored.

Based on their local persistency (Figure 7) we classified 8 nodes as permanently dry ($\boldsymbol{P}_i = 0$), 18 nodes as persistent ($\boldsymbol{P}_i = 1$) and 32 nodes as temporary ($0 < \boldsymbol{P}_i < 1$). The latter represented the nodes which changed their status at least one time during the study period (i.e., the dynamic portion of the network). The total accuracy of the hierarchical model was equal to 0.996, meaning that the 99.6% of the observations were correctly classified as wet or dry (Figure 6). The accuracy of the model at each node was represented by the nodewise accuracy which ranged between 0.56 and 1.00 with a mean of 0.98, while the time-wise accuracy of the model during each survey (visual survey or camera, or both) ranged between 0.88 and 1.00 with a mean of 0.99 (Figure 6). The model correctly classified the status of all the dry and persistent nodes during the study period, while incorrect classifications occurred at 15 of the 32 temporary nodes of the network. Of these 15 nodes, 5 were monitored by cameras while the other 10 were monitored by visual surveys.

We found that the local persistency of the nodes of Montecalvello exhibited a non-monotonic and highly heterogeneous pattern along the network (Figure 7a).

The observed spatial patterns of local persistency can be summarized as follows: temporary or dry nodes were located in most cases in the proximity of the headwater, while persistent nodes were preferentially placed in the middle portion of the stream. Again, temporary nodes were found near the outlet, where the contributing area was higher. As a result, the outlet (node 1) and some nodes connected to it in the physical space (e.g., node 24) showed more water presence temporal variability that some nodes located in the middle portion of the network, which instead had always been wet (e.g., nodes 30, 31, 32, 50, 51, 53). This implies that the outlet was in a lower position in the hierarchical chain, as compared to other nodes with lower contributing area. The activation/deactivation patterns exhibited an equally high complexity. The hierarchical order of all the nodes, which reflected the

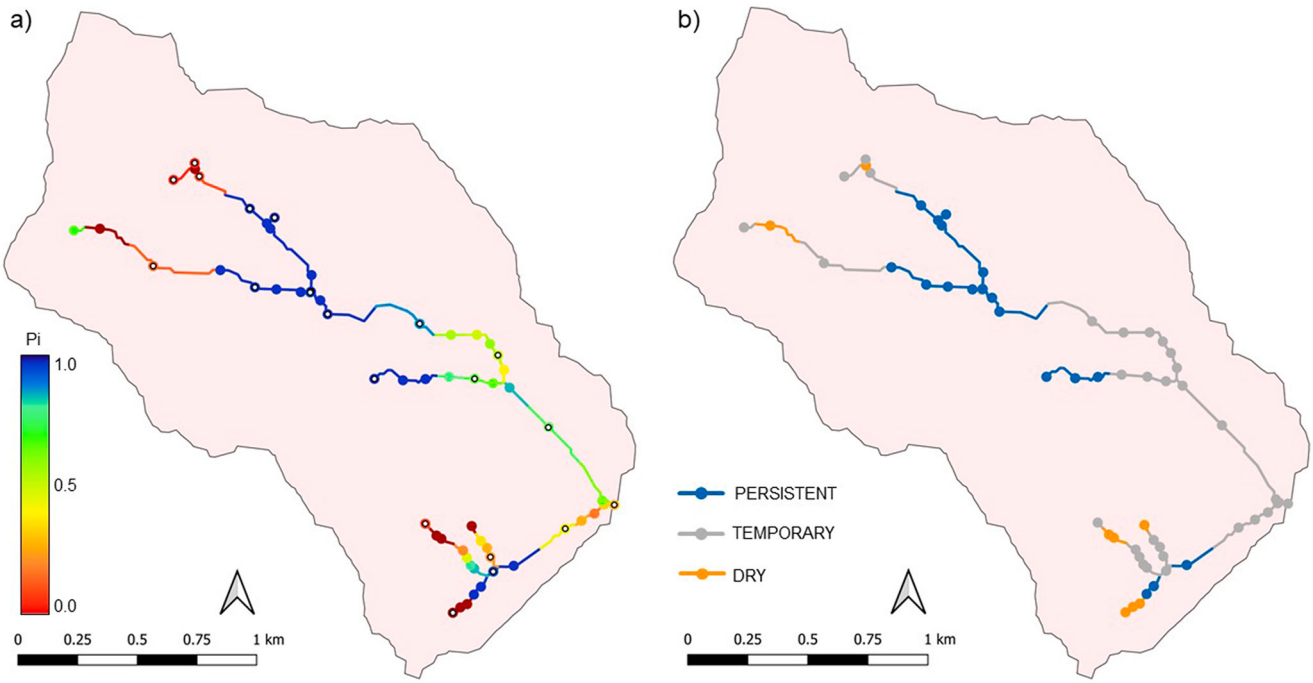

Figure 7. (a) Bayesian network of the Montecalvello catchment: nodes and stretches are colored based on their local persistency; white dots are nodes monitored by cameras. (b) Nodes and stretches classification based on their local persistency.

activation/deactivation order of Montecalvello catchment, is shown in Figure 6. An excerpt of the pattern of the modeled space-time dynamic of the Montecalvello catchment is shown in Figure 5.

The dry-down of the streams during summer typically started from nodes with higher contributing area and progressively expanded upstream. This behavior involved the lower and the middle parts of the catchment, leading however to a series of network disconnections in early summer (Figure 8). In particularly dry weather conditions (e.g., summer 2022) the wet stretch between the lower and the middle dry parts of the catchment also got dry. Then, the rewetting cycle started from upstream and then propagated downstream during fall. Expansion of the drainage network can be also found during summer, in which some nodes changed their status in response to short term rainfall (Figure 9). For instance, this is the case of the network expansion observed on 10 June 2021, during a rainfall with intensity of 45 mm/hr and duration of 1 hr (Figure 8).

4. Discussion

The main advantage of combining visual surveys and cameras is the ability of the proposed method to keep all the benefits of these two techniques (as compared to alternative tools such as water presence sensors and satellite images), though overcoming the key limits of these techniques taken separately (only cameras or only visual surveys). In particular, the proposed "combination" approach allows one to overcome the issue of recognizing no flow conditions from time series gathered by in situ sensors such as pressure transducers or water presence sensors, which might be problematic in case of soft river beds, complex water flow paths, erosion, and high sediment transport (Noto et al., 2022; Zanetti et al., 2022). Likewise, the proposed method eliminates the issues associated to the identification of the hydrological status of the streams from aerial images (taken with satellites or Uncrewed Aerial Vehicles), which is often problematic in case of dense riparian vegetation and limited streams width (Micieli et al., 2022). Moreover, the cameras have limited maintenance requirements: the batteries and the stick memories used allowed 1 month of continuous data acquisition (at least with the temporal frequency adopted in this study). Therefore, the visual surveys which were dedicated to the cameras' maintenance and data download could be significantly diluted in time, with a significant reduction of the empirical burden associated to manual operations. On the other hand, the limited temporal resolution of the visual surveys used in this study could have led to prolonged no-data periods, in case of technical issue occurring right after each maintenance inspection. However, the circumstance didn't happen frequently in our case study, owing the high reliability of the

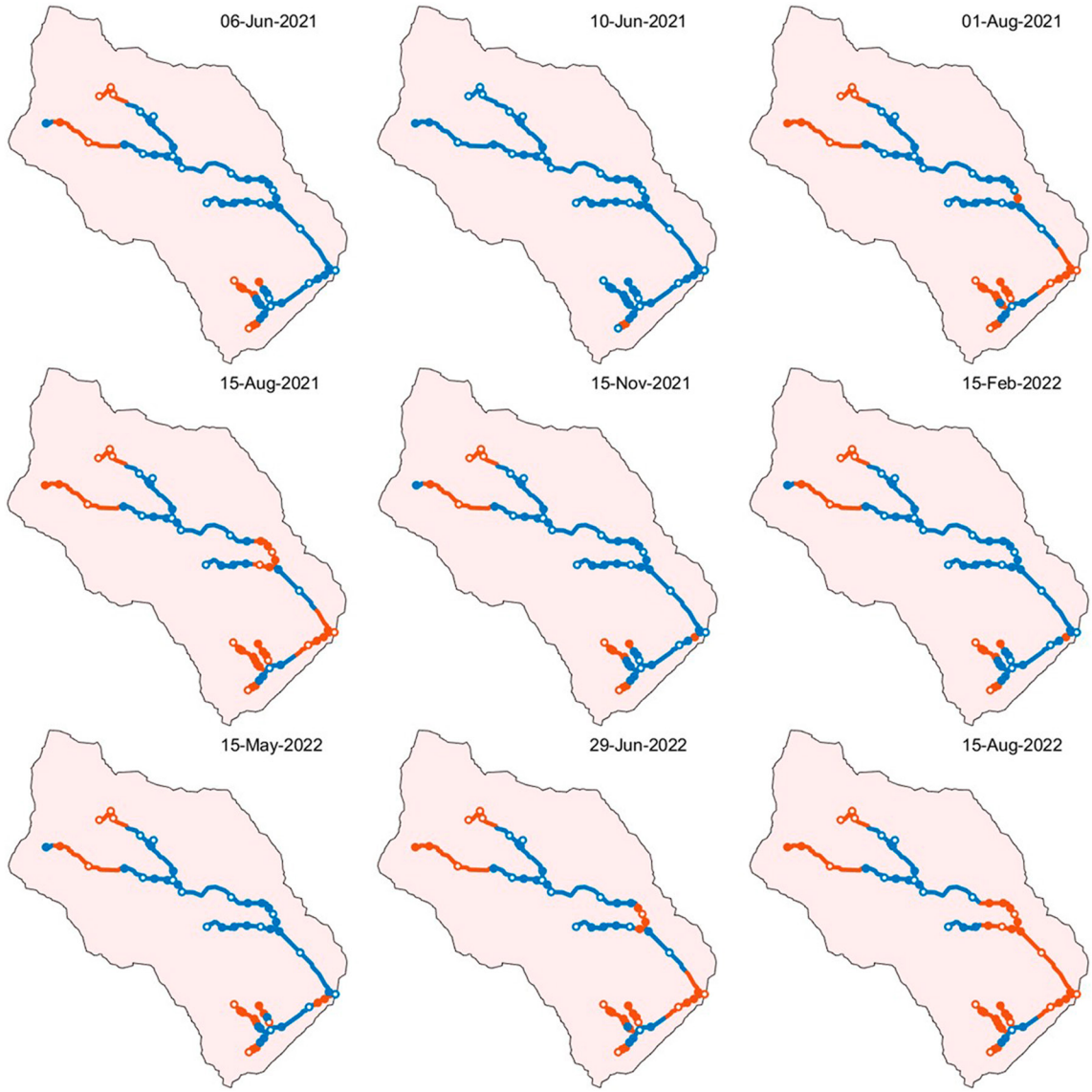

Figure 8. Space-time dynamics examples at Montecalvello catchment from June 2021 to August 2022: the modeled wet portion of the drainage network is represented by the blue line, while the dry stretches are represented by the orange line; the white dots represent the nodes monitored by cameras. Progressively drying phase from 6 June 2021 to 15 August 2021, with an isolated daily wet phase on 10 June 2021 during a heavy rainfall event (intensity = 45 mm/hr, duration = 1 hr). Then, the wetting phase and maximum extent of the network recorded in autumn and winter 2021–2022. Following, the drying phase during the summer 2022.

installed cameras. However, the observation matrix contains a huge amount of data about the state of the network during the study period, and is well suited to the application of the hierarchical principle to eliminate potential data gaps.

Despite the fact that the heterogeneity of the spatiotemporal resolution of the data collected in this study might be an issue in terms of data management, the use of the hierarchical principle makes possible to easily merge data sets with diverse characteristics, thereby reaching an optimal trade-off between empirical efforts, precision and amount of data to be managed. In fact, merging the data gathered from the combination of the visual surveys and cameras provided information on the whole network with a biweekly or monthly time resolution, while offering a high resolution view on the temporal dynamics on a selected subset of the network nodes. The high frequency continuous monitoring of some nodes improved the accuracy of the estimate of the local persistency therein, an instance which ensured a higher precision in the reconstruction of the hierarchy when combined with the data collected through visual surveys. Therefore, in the proposed "combination" method, the visual surveys increased

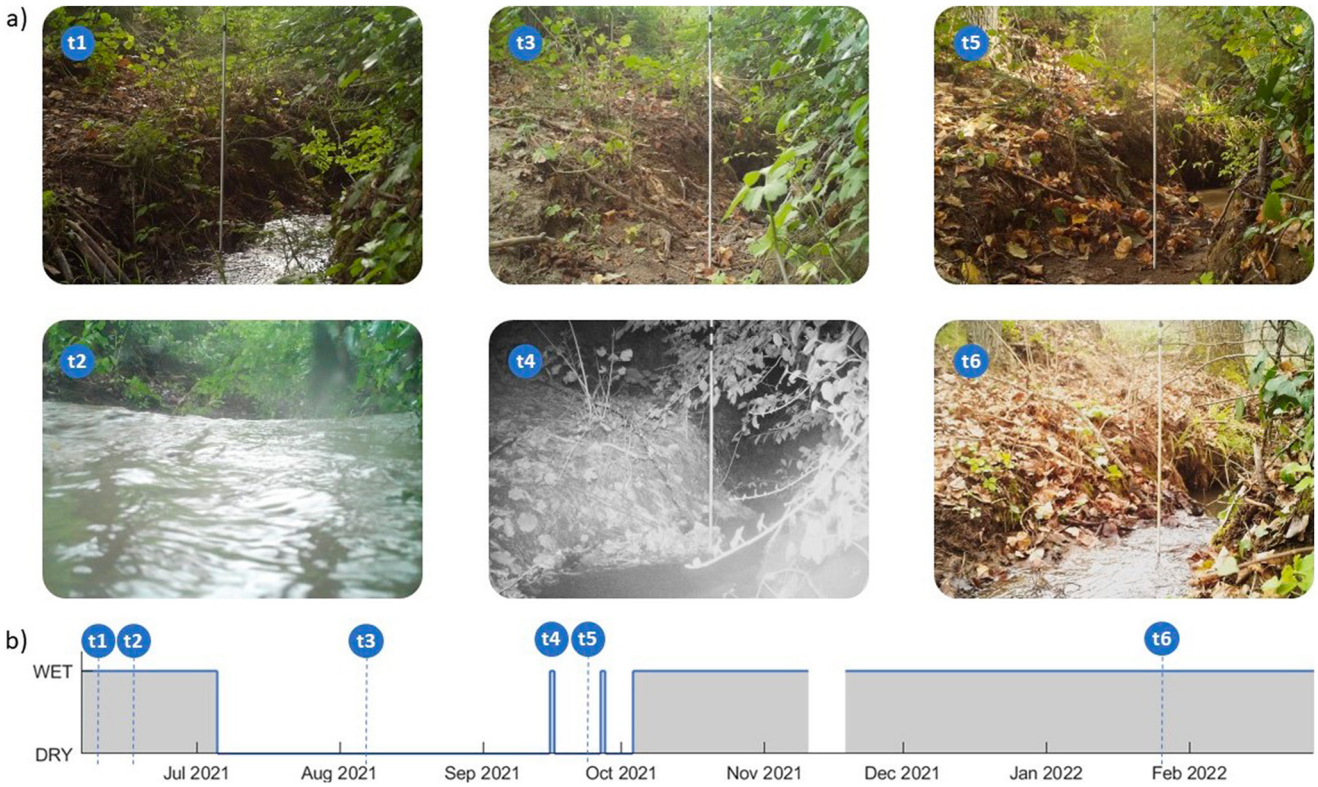

Figure 9. Example of monitoring of the streamflow state at node 1 through camera. (a) A few frames (t1-t6) captured during the study period. (b) Plot showing the temporal dynamic (wet or dry): t1 and t6 represent the streamflow state from fall to spring; t2 and t4 represent the state during rainfall events; t3 and t5 represent the state during the dry season. The data gap in the plot between November and December was due to maintenance issues.

the spatial coverage of the data set, while the cameras improved its temporal resolution in some nodes. Likewise, the hierarchical principle and the visual surveys allowed us to extrapolate in space the information collected with cameras. Figure 6 clearly shows the improvement in the ability to describe the underlying stream network dynamics when the two methods are combined (in the part of the plot below the yellow line) as compared to the initial part of the campaign, when only field surveys were used (in the part of the plot above the yellow line).

The homogenization of the two data sets, however, required some subjective criteria to create a homogeneous daily data set starting from heterogeneous sources. The visual surveys were in fact taken during randomly selected times of a given survey day, while the multiple sub-hourly images were gathered with the cameras during any individual day of the campaign. To create a daily data set, in this case, we assumed that each visual survey was able to represent the state of the network during the whole day in which the survey was conducted, regardless of the specific survey time. The assumption seems to be mild, as long visual surveys were mostly performed under stable weather conditions, a circumstance that enhances the stability of the flowing network. On the other hand, we decided to consider as wet, on a given day, a node that was observed as wet during at least one of the images collected by the cameras during that day. Normally, this choice is not expected to have a strong impact on the results, as the wetting and drying cycles experienced by the stream network are typically quite slow (especially in between rain events). In this specific case, however, the observed network dynamics indicated the presence of sub-daily dynamics in some nodes. Therefore, the criteria used to identify wet and dry days during the monitoring period could potentially impact the local results obtained therein. Nevertheless, it is difficult to identify the optimal criterion to define wet and dry days a priori, as any choice has its own limits and advantages. A key advantage was represented by the fact that the selected criterion was able to detect the daily wetting and drying cycles occurred in response to heavy rainfall events, as compared to the visual surveys which were generally performed with stable weather conditions. In any case, the technique used to define the daily state of each node affected the calculation of the local persistency only in a limited number of temporary nodes, and always to a negligible extent, because of the pronounced velocity of the wet/dry sub-daily cycles and the limited number of times in which such cycles occurred.

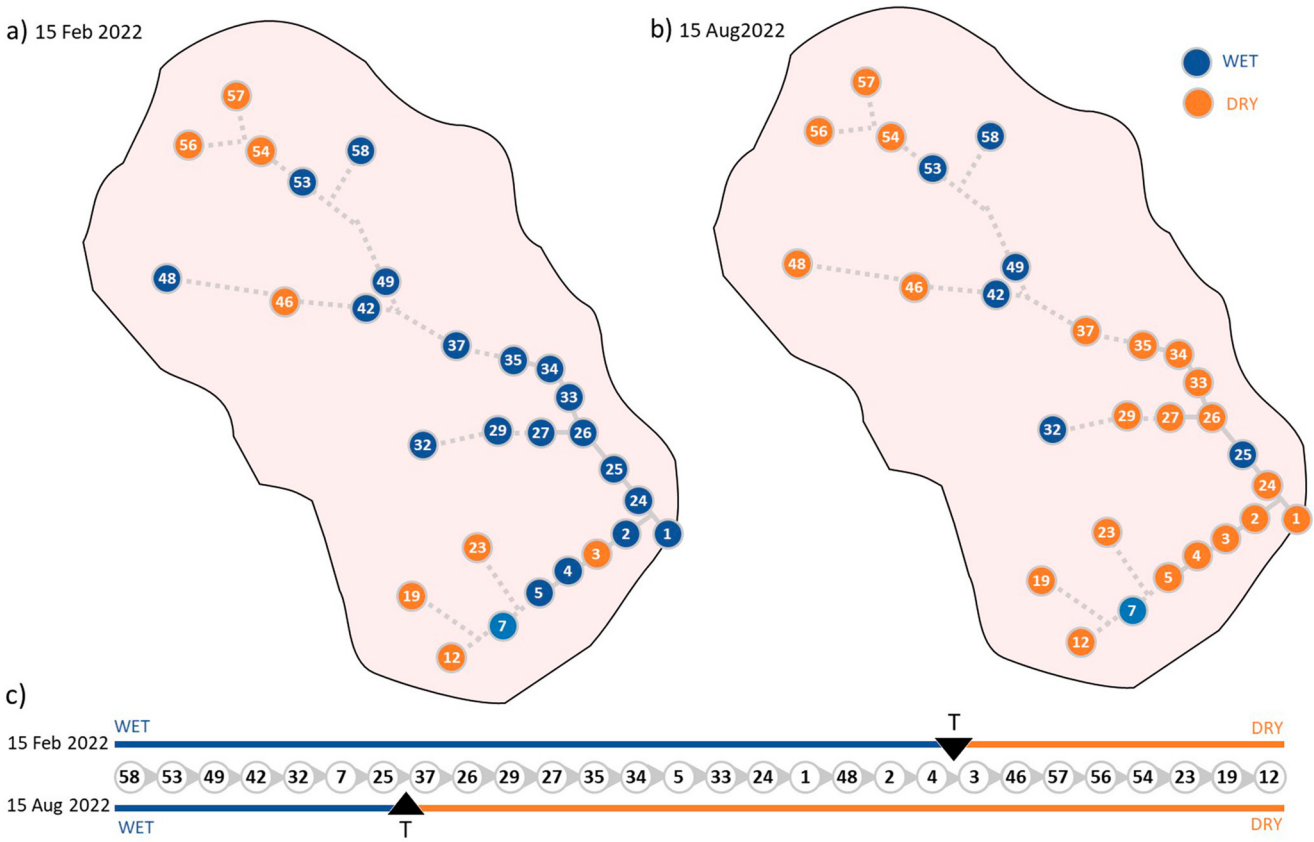

Figure 10. (a) Modeled states of some of the monitoring nodes during 15 February 2022. (b) Modeled states of the same nodes during 15 August 2022. (c) Comparison of the position of the threshold T along the chain of the nodes listed in the hierarchical order, from most (left) to least (right) persistent: the black arrows represent the time dependent thresholds that separated wet nodes (blue lines) from dry nodes (orange lines).

Potentially, the proposed experimental apparatus could be used to detect also isolated pools along the river network, which represent important biogeochemical hotspot of river system (Vander Vorste et al., 2020). However, considering the state of the network nodes as a binary random variable (wet/dry) is a very useful simplification to describe the spatiotemporal dynamics of non-perennial streams and their connectivity in most settings. Moreover, the separation between wet/dry/ponding conditions might not be operationally simple to define in some cases. In previous works pools were either considered as part of the wet nodes (Cunillera-Montcusí et al., 2023) or were excluded from the computation of the wet length of the network (Durighetto et al., 2020; Ilja Van Meerveld et al., 2019; Senatore et al., 2021). The latter seems to be a reasonable option, provided that only the flowing streams contribute to the active transport of water and matter downstream. Since the hierarchical model is based on the definition of the state of a node through a Bernullian, binary random variable incorporating the pools as a third potential state of a node seems to be quite challenging, as the basics of the hierarchical theory would need to be reformulated and revalidated. However, a significant number of pools along the network was not observed, with a few exception during the most severe dry periods. Therefore, this issue is left to forthcoming research.

The reconstruction of the wet portion of the network along the study period highlighted the complexity of the wetting/drying cycles of the Montecalvello. In fact, while the extent of the wet portion of the stream network contracted in summer and expanded in fall, as implied by Mediterranean climate, the spatial patterns of the wet portion of the network reflected the non-monotonic pattern of the local persistency of the nodes shown in Figure 7, leading to a dynamically fragmented drainage network. Figure 10 depicts the state of the nodes reconstructed exploiting the hierarchical principle in two different dates, one during the winter of 2022 and one during the summer of 2022.

In both maps shown in Figure 10, the network disconnections are clearly visible, as some dry nodes disconnect the upstream flowing network from other downstream wet nodes, including the outlet. The disconnections occurred both in winter and summer, while the number of dry nodes significantly increased in the latter case. Interestingly,

network contraction involved not only the headwaters, but also the lower and middle parts of the catchment. In some cases the dry-down originated from nodes with a relatively high contributing area and then propagated upstream. The observed spatiotemporal variability of active streams in the Montecalvello was found to be in line with previous studies conducted in Mediterranean catchments. For instance, in Llanos-Paez et al. (2023), the stream intermittency was particularly evident in a few small stream segments located in the upstream part of the network. Heterogeneity in the spatial patterns of local persistency, which implies disconnections in the active drainage network, were previously observed in humid settings (Durighetto et al., 2020) and Mediterranean climates (Senatore et al., 2021). In particular, Senatore et al. (2021) highlighted the dependency of persistency on stationary morphologic and geolithological features of a Mediterranean catchment, emphasizing the key role of evapotranspiration in the observed network contraction, which was confirmed by this study (as discussed below). In the Montecalvello, some temporary nodes are characterized by a lower contributing area (e.g., node 20), while others are characterized by a larger width of the streambed (e.g. nodes 34 and 1). The least persistent nodes in the network fall on the substrate classified as "gravel/conglomerate," which is characterized by a higher permeability—an instance that is known to increase the subsurface discharge capacity of a node, reducing the corresponding surface flow persistence (Durighetto & Botter, 2022). Quite surprisingly, some persistent nodes (e.g., nodes 40, 41, 42, 49, and 50) also rely on the same substrate, although some other nodes, characterized by higher persistency, fall on the substrate classified as "tufa/diatomite/clays." According to the lower hydraulic conductivity values associated to clay layers (Chen, 2004; Chen et al., 2013), we propose that the lower permeability attributable to clay substrates might contribute to increase the persistency of such nodes. The nodes which dry first are mainly located in the lower part of the catchment and they fall in the "gravel/conglomerate" class (Figure S4 in Supporting Information S1). An "intermittent stream flows in response to snowmelt and/or elevated groundwater tables resulting from increased periods of precipitation and/or decreased evapotranspiration" (McDonough et al., 2011), and it is hydrologically gaining the majority of time (Busch et al., 2020), while it is hydrologically losing during dry periods (McDonough et al., 2011). The evapotranspiration of the riparian zone affects groundwater level fluctuation (Butler et al., 2007) and it is one of the causes that lead to flow cessation and drying (Busch et al., 2020; McDonough et al., 2011). Actually, some of the temporary nodes, in particular the nodes which dry first, are located in the fraction of the network where riparian vegetation is more developed. Moreover, the downstream portion of the river network is characterized by lower slopes as compared to the upstream nodes, an instance that can facilitate the connectivity between surface and subsurface water and enhance the effect of evapotranspiration on surface flow presence. Thus, the combination of these hydrogeological conditions is likely to enhance the degree of temporariness of the nodes located in the downstream part of the network.

The observed dynamics of the Montecalvello river network suggested that the same hierarchical pattern is valid for the 3 monitored years (2020–2022). However, sporadic non-hierarchical behaviors of a few nodes of the network, which are represented by false positives (FP) and false negatives (FN) shown in Figure 6. Globally, FP and FN can be found during the drying and the wetting phases, although some isolated FP and FN can be found even during the dry and wet seasons. The presence of FP and FN implied that the state (wet vs. dry) of the nodes as imposed by the hierarchy during a certain survey didn't reflect the observed state of such nodes. For instance, this was the case of nodes 24, 1, 48, 21, 15, and 20 (listed here with a descending hierarchical order). The order according to which these nodes got dry in the summer 2021 did not exactly follow the sequence dictated by the hierarchical chain, as node 1 got dry first, followed by the least persistent ones (nodes 24, 15, 20, see Figure 6). We assume that this non-hierarchical behavior can be attributable a non-linearity in the hydrological response possibly emerging only during certain periods of the year, or the presence of specific hydrologic conditions observed only within the most intense dry periods.

In spite of the complexity of the processes driving the wetting and drying of the network in the Montecalvello site and the non-monotonic pattern of local persistency, the hierarchical model properly described the expansion and contraction dynamic of the network with a very high accuracy (>99%). Once the hierarchy is known based on information on the state of pairs of nodes in the network, it is possible to estimate the state of the entire network based on the inspection of a few strategic nodes. In fact, the hierarchical activation scheme allows the optimization of the number of monitored nodes: when a wet node is observed, all the more persistent nodes must be wet too, opposite, when a dry node is observed, all the less persistent nodes must be dry. This implies that much smaller number of nodes need to be inspected in any survey. While the application of the hierarchical principle represents a useful tool for reconstructing the active portion of the network, allowing the definition of the state of each node in the network based on the inspection of a few nodes, several observation of the state of all the

nodes in the network (or some of them) are needed to construct the hierarchy. Experimental data is always key to enhance understanding of hydrological processes, but is particularly important in complex environments such as the Montecalvello catchment, in which the spatial heterogeneity of the observed stream dynamics was particularly pronounced. In this context the use of cameras represents a useful tool to obtain long-term information about the observed state on some key nodes and it remains the only technique available to provide information about spatially distributed runoff dynamics in response to short-term rain events.

5. Conclusions

In this work the data gathered using two different methods (cameras and visual surveys) with heterogeneous spatial and temporal resolutions, were merged exploiting the hierarchical principle. This combination method was applied to reconstruct the spatiotemporal stream dynamics of a Mediterranean intermittent catchment of central Italy. The following conclusions are worth emphasizing:

- The proposed method, consisting on merging data from visual surveys and cameras, was able to keep all the advantages of each technique—namely the high temporal resolution of the cameras and the high spatial resolution of visual surveys—and overcame the limits of the above methods taken separately, thereby allowing an accurate description of the spatiotemporal dynamics of the Montecalvello stream network.
- The reconstruction of the spatiotemporal dynamics of stream network exploiting the hierarchical principle highlighted the complexity of the patterns of drying/wetting cycles in the Montecalvello. The wet portions of the stream network contracted during summer and expanded in fall with a highly heterogeneous spatial patterns, which led to important dynamical disconnections along the main stream and the tributaries. The set of factors such as geology, morphology, and vegetation cover could be one of the various potential factors which explain the observed pattern dynamic in the montecalvello catchment.
- Despite the above complexity, the observed stream network dynamics in the Montecalvello catchment were in line with previous studies conducted in similar climatic settings, and they followed the hierarchical principle, with a mean accuracy of the hierarchical model of 99.6%.
- The cameras were found to be a useful tool to support other traditional methods to gather experimental data about the hierarchy of the stream network, especially in conditions in which the monitoring is particularly challenging. Once the hierarchy of the stream is known, it is possible to estimate the states of the entire network through the inspection of a few nodes. This facilitates the monitoring of stream network dynamics in complex and difficult-to-access environments such as the Montecalvello.

Data Availability Statement

The data used in this study is publicly available at https://researchdata.cab.unipd.it/id/eprint/831.

Acknowledgments
This research was supported by the European Community's Horizon 2020 Excellent Science Programme (Grant H2020-EU.1.1.-770999). We thank Arianna Canini, David Busetti, Roberto Giulianelli, Camilla Bacoccoli, Angelo Orlando, and Linda Cisamolo for their help in instruments maintenance and in performing the surveys.

References

Assendelft, R., & van Meerveld, H. J. (2019). A low-cost, multi-sensor system to monitor temporary stream dynamics in mountainous headwater catchments. *Sensors*, *19*(21), 4645. https://doi.org/10.3390/s19214645

Banegas-Medina, A., Montes, I. Y., Tzoraki, O., Brendonck, L., Pinceel, T., Diaz, G., et al. (2021). Hydrological, environmental and taxonomical heterogeneity during the transition from drying to flowing conditions in a Mediterranean intermittent river. *Biology*, *10*(4), 316. https://doi.org/10.3390/BIOLOGY10040316

Borg Galea, A., Sadler, J. P., Hannah, D. M., Datry, T., & Dugdale, S. J. (2019). Mediterranean intermittent rivers and ephemeral streams: Challenges in monitoring complexity. In *Ecohydrology* (Vol. 12). John Wiley and Sons Ltd. https://doi.org/10.1002/eco.2149

Botter, G., & Durighetto, N. (2020). The stream length duration curve: A tool for characterizing the time variability of the flowing stream length. *Water Resources Research*, *56*(8), e2020WR027282. https://doi.org/10.1029/2020WR027282

Botter, G., Vingiani, F., Senatore, A., Jensen, C., Weiler, M., McGuire, K., et al. (2021). Hierarchical climate-driven dynamics of the active channel length in temporary streams. *Scientific Reports*, *11*(1), 21503. https://doi.org/10.1038/s41598-021-00922-2

Burrows, R. M., Rutlidge, H., Bond, N. R., Eberhard, S. M., Auhl, A., Andersen, M. S., et al. (2017). High rates of organic carbon processing in the hyporheic zone of intermittent streams. *Scientific Reports*, *7*(1), 1–11. https://doi.org/10.1038/s41598-017-12957-5

Busch, M. H., Costigan, K. H., Fritz, K. M., Datry, T., Krabbenhoft, C. A., Hammond, J. C., et al. (2020). What's in a name? Patterns, trends, and suggestions for defining non-perennial rivers and streams. *Water*, *12*(7), 1980. https://doi.org/10.3390/w12071980

Butler, J. J., Kluitenberg, G. J., Whittemore, D. O., Loheide, S. P., Jin, W., Billinger, M. A., & Zhan, X. (2007). A field investigation of phreatophyte-induced fluctuations in the water table. *Water Resources Research*, *43*(2), 2404. https://doi.org/10.1029/2005WR004627

Chen, X. (2004). Streambed hydraulic conductivity for rivers in south-central Nebraska. *Journal of the American Water Resources Association*, *40*(3), 561–573. https://doi.org/10.1111/j.1752-1688.2004.tb04443.x

Chen, X., Dong, W., Ou, G., Wang, Z., & Liu, C. (2013). Gaining and losing stream reaches have opposite hydraulic conductivity distribution patterns. *Hydrology and Earth System Sciences*, *17*(7), 2569–2579. https://doi.org/10.5194/HESS-17-2569-2013

Constantz, J. (2008). Heat as a tracer to determine streambed water exchanges. *Water Resources Research*, *44*(4), W00D10. https://doi.org/10.1029/2008WR006996

Costigan, K. H., Kennard, M. J., Leigh, C., Sauquet, E., Datry, T., & Boulton, A. J. (2017). Flow regimes in intermittent rivers and ephemeral streams. In *Intermittent rivers and ephemeral streams* (pp. 51–78). Elsevier. https://doi.org/10.1016/B978-0-12-803835-2.00003-6

Cunillera-Montcusí, D., Fernández-Calero, J. M., Pölsterl, S., Argelich, R., Fortuño, P., Cid, N., et al. (2023). Navigating through space and time: A methodological approach to quantify spatiotemporal connectivity using stream flow data as a case study. *Methods in Ecology and Evolution*, *14*(7), 1780–1795. https://doi.org/10.1111/2041-210X.14105

Datry, T., Larned, S. T., & Tockner, K. (2014). Intermittent rivers: A challenge for freshwater ecology. *BioScience*, *64*(3), 229–235. https://doi.org/10.1093/biosci/bit027

Durighetto, N., Bertassello, L. E., & Botter, G. (2022). Eco-hydrological modelling of channel network dynamics—Part 1: Stochastic simulation of active stream expansion and retraction. *Royal Society Open Science*, *9*(11). https://doi.org/10.1098/rsos.220944

Durighetto, N., & Botter, G. (2022). On the relation between active network length and catchment discharge. *Geophysical Research Letters*, *49*(14), e2022GL099500. https://doi.org/10.1029/2022GL099500

Durighetto, N., Vingiani, F., Bertassello, L. E., Camporese, M., & Botter, G. (2020). Intraseasonal drainage network dynamics in a headwater catchment of the Italian Alps. *Water Resources Research*, *56*(4), e2019WR025563. https://doi.org/10.1029/2019WR025563

Giezendanner, J., Benettin, P., Durighetto, N., Botter, G., & Rinaldo, A. (2021). A note on the role of seasonal expansions and contractions of the flowing fluvial network on metapopulation persistence. *Water Resources Research*, *57*(11), e2021WR029813. https://doi.org/10.1029/2021WR029813

Godsey, S. E., & Kirchner, J. W. (2014). Dynamic, discontinuous stream networks: Hydrologically driven variations in active drainage density, flowing channels and stream order. *Hydrological Processes*, *28*(23), 5791–5803. https://doi.org/10.1002/HYP.10310

Gómez-Gener, L., Siebers, A. R., Arce, M. I., Arnon, S., Bernal, S., Bolpagni, R., et al. (2021). Towards an improved understanding of biogeochemical processes across surface-groundwater interactions in intermittent rivers and ephemeral streams. *Earth-Science Reviews*, *220*, 103724. https://doi.org/10.1016/J.EARSCIREV.2021.103724

Herzog, A., Stahl, K., Veit, B., & Weiler, M. (2022). Measuring zero water level in stream reaches: A comparison of an image-based versus a conventional method. *Hydrological Processes*, *36*(8), e14658. https://doi.org/10.1002/HYP.14658

Ilja Van Meerveld, H. J., Kirchner, J. W., Vis, M. J. P., Assendelft, R. S., & Seibert, J. (2019). Expansion and contraction of the flowing stream network alter hillslope flowpath lengths and the shape of the travel time distribution. *Hydrology and Earth System Sciences*, *23*(11), 4825–4834. https://doi.org/10.5194/HESS-23-4825-2019

Jensen, C. K., McGuire, K. J., & Prince, P. S. (2017). Headwater stream length dynamics across four physiographic provinces of the Appalachian Highlands. *Hydrological Processes*, *31*(19), 3350–3363. https://doi.org/10.1002/hyp.11259

Jensen, C. K., McGuire, K. J., Shao, Y., & Dolloff, C. A. (2018). Modeling wet headwater stream networks across multiple flow conditions in the Appalachian Highlands. *Earth Surface Processes and Landforms*, *43*(13), 2762–2778. https://doi.org/10.1002/ESP.4431

Kaplan, N. H., Sohrt, E., Blume, T., & Weiler, M. (2019). Monitoring ephemeral, intermittent and perennial streamflow: A dataset from 182 sites in the Attert catchment, Luxembourg. *Earth System Science Data*, *11*(3), 1363–1374. https://doi.org/10.5194/essd-11-1363-2019

Kirkby, M., Callan, J., Weyman, D., & Wood, J. (1976). Measurement and modelling of dynamic contributing areas in very small catchments. In *Working paper no. 167*. School of Geography, University of Leeds.

Koski, T., & Noble, J. M. (2011). *Bayesian networks: An introduction*. Wiley.

Lapides, D. A., Leclerc, C. D., Moidu, H., Dralle, D. N., & Hahm, W. J. (2021). Variability of stream extents controlled by flow regime and network hydraulic scaling. *Hydrological Processes*, *35*(3). https://doi.org/10.1002/HYP.14079

Larned, S. T., Datry, T., Arscott, D. B., & Tockner, K. (2010). Emerging concepts in temporary-river ecology. *Freshwater Biology*, *55*(4), 717–738. https://doi.org/10.1111/J.1365-2427.2009.02322.X

Leigh, C., Boulton, A. J., Courtwright, J. L., Fritz, K., May, C. L., Walker, R. H., & Datry, T. (2016). Ecological research and management of intermittent rivers: An historical review and future directions. *Freshwater Biology*, *61*(8), 1181–1199. https://doi.org/10.1111/fwb.12646

Llanos-Paez, O., Estrada, L., Pastén-Zapata, E., Boithias, L., Jorda-Capdevila, D., Sabater, S., & Acuña, V. (2023). Spatial and temporal patterns of flow intermittency in a Mediterranean basin using the SWAT+ model. *Hydrological Sciences Journal*, *68*(2), 276–289. https://doi.org/10.1080/02626667.2022.2155523

McDonough, O. T., Hosen, J. D., & Palmer, M. A. (2011). Temporary streams: The hydrology, geography, and ecology of non-perennially flowing waters. In *River ecosystems: Dynamics, management and conservation* (pp. 259–290). Retrieved from https://www.researchgate.net/publication/285964976_Temporary_streams_The_hydrology_geography_and_ecology_of_non-perennially_flowing_waters

Messager, M. L., Lehner, B., Cockburn, C., Lamouroux, N., Pella, H., Snelder, T., et al. (2021). Global prevalence of non-perennial rivers and streams. *Nature*, *594*(7863), 391–397. https://doi.org/10.1038/s41586-021-03565-5

Micieli, M., Botter, G., Mendicino, G., & Senatore, A. (2022). UAV thermal images for water presence detection in a Mediterranean headwater catchment. *Remote Sensing*, *14*(1), 108. https://doi.org/10.3390/RS14010108

Miliša, M., Stubbington, R., Datry, T., Cid, N., Bonada, N., Šumanović, M., & Milošević, D. (2022). Taxon-specific sensitivities to flow intermittence reveal macroinvertebrates as potential bioindicators of intermittent rivers and streams. *Science of the Total Environment*, *804*, 150022. https://doi.org/10.1016/j.scitotenv.2021.150022

Noto, S., Tauro, F., Petroselli, A., Apollonio, C., Botter, G., & Grimaldi, S. (2022). Low-cost stage-camera system for continuous water-level monitoring in ephemeral streams. *Hydrological Sciences Journal*, *67*(9), 1–10. https://doi.org/10.1080/02626667.2022.2079415

Pastor, A. V., Tzoraki, O., Bruno, D., Kaletová, T., Mendoza-Lera, C., Alamanos, A., et al. (2022). Rethinking ecosystem service indicators for their application to intermittent rivers. *Ecological Indicators*, *137*, 108693. https://doi.org/10.1016/j.ecolind.2022.108693

Peirce, S. E., & Lindsay, J. B. (2015). Characterizing ephemeral streams in a southern Ontario watershed using electrical resistance sensors. *Hydrological Processes*, *29*(1), 103–111. https://doi.org/10.1002/hyp.10136

Prancevic, J. P., & Kirchner, J. W. (2019). Topographic controls on the extension and retraction of flowing streams. *Geophysical Research Letters*, *46*(4), 2084–2092. https://doi.org/10.1029/2018GL081799

Rivas-Martínez, S., Sáenz, S., & Penas, A. (2011). Worldwide bioclimatic classification system. *Global Geobotany*, *1*, 1–634+4. Maps. https://doi.org/10.5616/gg110001

Sarremejane, R., Messager, M. L., & Datry, T. (2021). Drought in intermittent river and ephemeral stream networks. *Ecohydrology*, *15*(5). https://doi.org/10.1002/ECO.2390

Senatore, A., Micieli, M., Liotti, A., Durighetto, N., Mendicino, G., & Botter, G. (2021). Monitoring and modeling drainage network contraction and dry down in Mediterranean headwater catchments. *Water Resources Research*, *57*(6), e2020WR028741. https://doi.org/10.1029/2020WR028741

Serrano-Notivoli, R., Martínez-Salvador, A., García-Lorenzo, R., Espín-Sánchez, D., & Conesa-García, C. (2022). Rainfall–runoff relationships at event scale in western Mediterranean ephemeral streams. *Hydrology and Earth System Sciences*, *26*(5), 1243–1260. https://doi.org/10.5194/HESS-26-1243-2022

Spence, C., Mengistu, S., & Spence, C. (2015). Deployment of an unmanned aerial system to assist in mapping an intermittent stream. https://doi.org/10.1002/hyp.10597

Steward, A. L., Datry, T., & Langhans, S. D. (2022). The terrestrial and semi-aquatic invertebrates of intermittent rivers and ephemeral streams. *Biological Reviews*, *97*(4), 1408–1425. https://doi.org/10.1111/BRV.12848

Stubbington, R., Acreman, M., Acuña, V., Boon, P. J., Boulton, A. J., England, J., et al. (2020). Ecosystem services of temporary streams differ between wet and dry phases in regions with contrasting climates and economies. *People and Nature*, *2*(3), 660–677. https://doi.org/10.1002/pan3.10113

Tauro, F., Noto, S., Botter, G., & Grimaldi, S. (2022). Assessing the optimal stage-cam target for continuous water level monitoring in ephemeral streams: Experimental evidence. *Remote Sensing*, *14*(23), 6064. https://doi.org/10.3390/rs14236064

Tooth, S. (2000). Process, form and change in dryland rivers: A review of recent research. *Earth-Science Reviews*, *51*(1–4), 67–107. https://doi.org/10.1016/S0012-8252(00)00014-3

Tulbure, M. G., Broich, M., Perin, V., Gaines, M., Ju, J., Stehman, S. V., et al. (2022). Can we detect more ephemeral floods with higher density harmonized Landsat Sentinel 2 data compared to Landsat 8 alone? *ISPRS Journal of Photogrammetry and Remote Sensing*, *185*, 232–246. https://doi.org/10.1016/J.ISPRSJPRS.2022.01.021

Vander Vorste, R., Sarremejane, R., & Datry, T. (2020). Intermittent rivers and ephemeral streams: A unique biome with important contributions to biodiversity and ecosystem services. In *Encyclopedia of the world's biomes* (pp. 419–429). Elsevier. https://doi.org/10.1016/B978-0-12-409548-9.12054-8

Vertessy, R. A., & Elsenbeer, H. (1999). Distributed modeling of storm flow generation in an Amazonian rain forest catchment: Effects of model parameterization. *Water Resources Research*, *35*(7), 2173–2187. https://doi.org/10.1029/1999WR900051

Zanetti, F., Durighetto, N., Vingiani, F., & Botter, G. (2022). Technical note: Analyzing river network dynamics and the active length-discharge relationship using water presence sensors. *Hydrology and Earth System Sciences*, *26*(13), 3497–3516. https://doi.org/10.5194/HESS-26-3497-2022

Zimmer, M. A., Kaiser, K. E., Blaszczak, J. R., Zipper, S. C., Hammond, J. C., Fritz, K. M., et al. (2020). *Zero or not? Causes and consequences of zero-flow stream gage readings*. Wiley Interdisciplinary Reviews: Water. https://doi.org/10.1002/wat2.1436

Zimmermann, B., Zimmermann, A., Turner, B. L., Francke, T., & Elsenbeer, H. (2014). Connectivity of overland flow by drainage network expansion in a rain forest catchment. *Water Resources Research*, *50*(2), 1457–1473. https://doi.org/10.1002/2012WR012660